Soil Dynamics and Earthquake Engineering 124 (2019) 162–171

Contents lists available at ScienceDirect

Soil Dynamics and Earthquake Engineering

journal homepage: www.elsevier.com/locate/soildyn

Post-cyclic volumetric strain of calcareous sand using hollow cylindrical torsional shear tests

Habib Shahnazari[a,*], Reza Rezvani[b], Mohammad Amin Tutunchian[c]

[a] School of Civil Engineering, Iran University of Science and Technology, P.O. Box 16765-163, Narmak, Tehran, Iran
[b] Faculty of Technology and Engineering, East of Guilan, University of Guilan, P.O. Box 44918-98566, Rudsar, Iran
[c] Payame Noor University, P.O. Box 19395-3697, Tehran, Iran

ARTICLE INFO

Keywords:
Hollow torsional shear test
Post-cyclic settlement
Post-cyclic volumetric strain
Calcareous sand

ABSTRACT

Post-cyclic settlement of saturated soil, due to dynamic loadings such as earthquake, causes severe damage to structures. Dissipation of excess pore water pressure generated during cyclic loadings results in the volumetric strain of soil materials. Many studies have been conducted on factors affecting post-cyclic volumetric strain ($\varepsilon_{re,v}$) of siliceous soils. The effect of important factors on post-cyclic settlement of calcareous sand is evaluated in this study. Calcareous soils are generally located in tropical and subtropical areas near oceans and gulfs. These deposits are usually saturated and consequently, post-cyclic settlement can be critical in these sediments. In this research, a series of hollow cylindrical torsional shear tests were performed on Hormuz calcareous sands obtained from the north coast of the Persian Gulf. The samples were loaded cyclically under different cyclic stress ratios (*CSRs*) in undrained condition and then, terminated at a desired pore water pressure ratio (r_u). After that, the excess pore water pressure was allowed to dissipate, and volumetric strain occurred as a result. The effects of relative density (*Dr*), cyclic stress ratio (*CSR*), excess pore water pressure ratio (r_u) and maximum cyclic-induced shear strain (γ_{max}) on $\varepsilon_{re,v}$ of the reconstituted sand were evaluated. The results showed that maximum shear strain is the most effective factor in estimating the post-cyclic settlement of the calcareous sand.

1. Introduction

Cyclic-induced deformation caused by dynamic loadings such as earthquakes can be divided into two categories: shear deformation and volume change. During dynamic loadings, pore water pressure increases in saturated soils. The liquefaction phenomenon occurs in cases of level- or mildly-sloping grounds, when the pore water pressure increases to the confining pressure in saturated soils during an earthquake. After that, excess pore water pressure dissipates and volume change takes place in the soil mass. These volume changes manifest as settlement in ground surface. Liquefaction may also cause sand boil, loss of bearing capacity, lateral spreading, etc. [1,2].

As reported by many researchers in different case studies and experimental investigations in siliceous deposits, excess pore water pressure dissipation causes cyclic-induced settlement. Retamal and Kausel [3] stated that the settlement was about 80 cm in some regions and was a result of soil densification after the Chile earthquake (1960). The cyclic-induced volumetric strain during the Niigata earthquake (1964) was reported to be about 3–5% [4]. Some regions experienced a 50 cm ground surface settlement after the earthquake, which resulted in significant damages. The non-homogenous nature of soils causes post-cyclic differential settlements that result in severe structural damages. Non-uniform settlements and structural damages were reported in many earthquakes such as the Niigata earthquake in Japan (1964) [5], the Luzon earthquake in the Philippines (1990) [6], the Kocaeli earthquake in Turkey (1995) [7], the Christchurch earthquake in New Zealand (2011) [8] and the Tohoku earthquake in Japan (2011) [9], all of which occurred in regions with siliceous soils.

Many experimental and semi-empirical studies have been conducted in estimating the post-cyclic volumetric strain ($\varepsilon_{re,v}$) in saturated siliceous soils. Lee and Albaisa [10] conducted an experimental study and showed that confining pressure, relative density, excess pore water pressure and soil particle shape are all factors that affect the $\varepsilon_{re,v}$. They also stated that according to the data, high scatter occurs after initial liquefaction, which corresponds to the failure condition. Nagase and Ishihara [4] performed a series of simple shear tests on Fuji river sand. The results showed a good relationship between the excess pore water pressure ratio (i.e., r_u, where $r_u = \Delta u/\sigma'_0$; Δu is excess pore water pressure and σ'_0 is initial effective stress) and post-cyclic volumetric strain ($\varepsilon_{re,v}$). The effect of relative density on $\varepsilon_{re,v}$ showed that

* Corresponding author.
E-mail addresses: hshahnazari@iust.ac.ir (H. Shahnazari), rezvani@guilan.ac.ir (R. Rezvani), amin@pnu.ac.ir (M.A. Tutunchian).

https://doi.org/10.1016/j.soildyn.2019.05.030
Received 27 December 2016; Received in revised form 11 January 2019; Accepted 18 May 2019
Available online 01 June 2019

Nomenclature

CO_2	carbon dioxide
CSR	cyclic stress ratio
CPT	cone penetration test
C_c	coefficient of curvature
C_u	coefficient of uniformity
Dr	relative density
Dr_{ac}	after consolidation relative density
D_{10}	soil diameter corresponding to 10% finer (effective grain size)
D_{30}	soil diameter corresponding to 30% finer
D_{50}	soil diameter corresponding to 50% finer
D_{60}	soil diameter corresponding to 60% finer
e_{max}	maximum void ratio
e_{min}	minimum void ratio
$\varepsilon_{re,v}$, ε_v	post-cyclic volumetric strain
Fe_2O_3	Iron (III) oxide
FS_L	factor of safety against liquefaction
G_s	specific gravity
$(\gamma_d)_{min}$	minimum dry density
$(\gamma_d)_{max}$	maximum dry density
γ_{max}	maximum single amplitude cyclic-induced shear strain
HCL	hydrochloric acid
$HI\ sand$	Hormuz Island sand
N_1	Japanese standard penetration value
N_{cyc}	number of cycles
q_{c1}	cone penetration value
r_u	excess pore water pressure ratio
SEM	scanning electron microscopic
SiO_2	silica
SPT	standard penetration test
S_v	vertical displacement of ground surface
σ_d	the amplitude of axial stress of cyclic loading
σ_{dL}	axial stress required for occurrence of initial liquefaction
σ'_0	initial effective stress
u_r	residual excess pore water pressure
Vs	shear wave velocity
z	thickness of the soil layers
Δr_u	variation of excess pore water pressure ratio
Δu	excess pore water pressure

increasing soil density decreases the post-cyclic settlement [4,11,12]. As shown in Fig. 1 and as confirmed by many researchers [10,13,14], when r_u reaches 1.0 (i.e., initial liquefaction condition), the $\varepsilon_{re,v}$ increases rapidly. Since the excess pore water pressure ratio cannot be greater than the unit value, some researchers did not find r_u to be a proper factor in estimating the $\varepsilon_{re,v}$ in liquefaction condition [4,15,16].

Shamoto et al. [16] introduced a method to estimate the settlement of saturated soil material after cyclic loadings. They stated that the maximum shear strain of soil induced by cyclic loading plays an important role in $\varepsilon_{re,v}$. Cyclic triaxial tests were conducted on Ottawa sand to evaluate the effect of confining pressures on $\varepsilon_{re,v}$ [17]. Ottawa sand samples were prepared at constant density and were consolidated at different confining pressures of 100, 300 and 400 kPa. The results showed that at a constant r_u level, increasing the confining pressures leads to higher $\varepsilon_{re,v}$ values. Lee and Albaisa [10] presented similar results about the effect of confining pressures on $\varepsilon_{re,v}$.

In semi-empirical methods, well-known field tests on siliceous soil such as the standard penetration test (*SPT*), cone penetration test (*CPT*) and shear wave velocity (V_s) were used to estimate the post-cyclic settlement of soils [11,15,18–20]. Ishihara and Yoshimine [15] proposed one of the well-known methods in estimating the $\varepsilon_{re,v}$ of terrigenous sediment (which are derived from the erosion of rocks). This method uses the following equation to calculate the factor of safety against liquefaction:

$$FS_L = \frac{(\sigma_{dL}/2\sigma'_0)_{20}}{(\sigma_d/2\sigma'_0)_{20}} \quad \text{(Eq.1)}$$

where FS_L is the factor of safety against liquefaction, σ_{dL} is the axial stress required to cause initial liquefaction (i.e., 5% double-amplitude axial strain in 20 cycles), σ_d is the amplitude of the axial stress corresponding to the cyclic loading and σ'_0 is the initial effective stress. To estimate the $\varepsilon_{re,v}$, the physical and mechanical properties of soil should be obtained in terms of the relative density (Dr), the maximum shear strain induced by earthquake (γ_{max}) and the Japanese standard penetration value (N_1) or cone penetration value (q_{c1}) (see Fig. 2).

Assuming the total surface subsidence is equivalent to sum of volumetric strain of the soil layers, ground surface settlement can be calculated by the following equation:

$$S_v = \int_0^z \varepsilon_{re,v}\, dz \quad \text{(Eq.2)}$$

where S_v is the vertical displacement of ground surface (or ground settlement), z is the thickness of the soil layers and $\varepsilon_{re,v}$ is the post-cyclic volumetric strain of soil layers obtained from different methods such as the method introduced by Ishihara and Yoshimine [15]. Previous studies have shown that when the factor of safety against liquefaction decreases to a threshold value, the $\varepsilon_{re,v}$ will be constant. This threshold value depends on the soil material properties [4,15,20,21].

While there are extensive researches on post-cyclic settlement of terrigenous soils, not much research has been done on the $\varepsilon_{re,v}$ evaluation of calcareous deposits. Calcareous deposits are generally located in tropical and subtropical areas such as the Persian Gulf, Hawaiian Islands, Puerto Rico, Republic of Ireland, and Australia. Calcareous sediments cover approximately 40% of the ocean's surface [22]. There are many differences between the mechanical behavior of calcareous and siliceous soils, which were reported in many researches [23–26]. Although calcareous sediments have higher internal friction angle due to shape and roughness of particles [23], the critical or ultimate state of these deposits is obtained in higher strain than that of siliceous soil [27,28]. Crushing of calcareous particles affects the mechanical behavior of this deposits [29–31]. As an instance, particle breakage increases the contractive behavior of carbonate samples [26,32]. Soil density, particle shape, gradation curve, stress and strain states and drainage

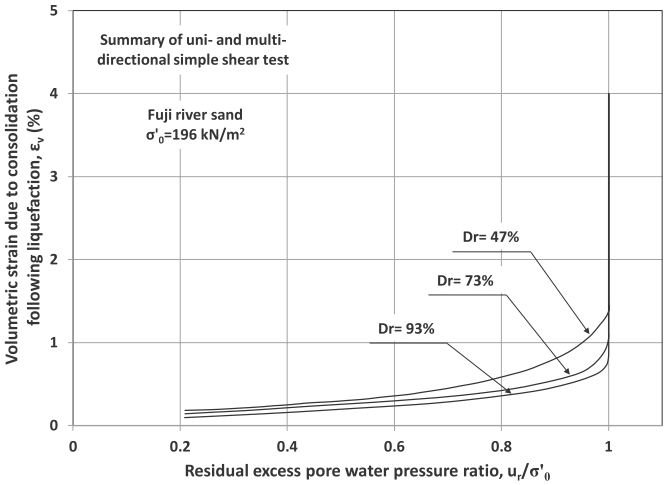

Fig. 1. The effect of relative density on post-cyclic volumetric strain of Fuji river sand [4].

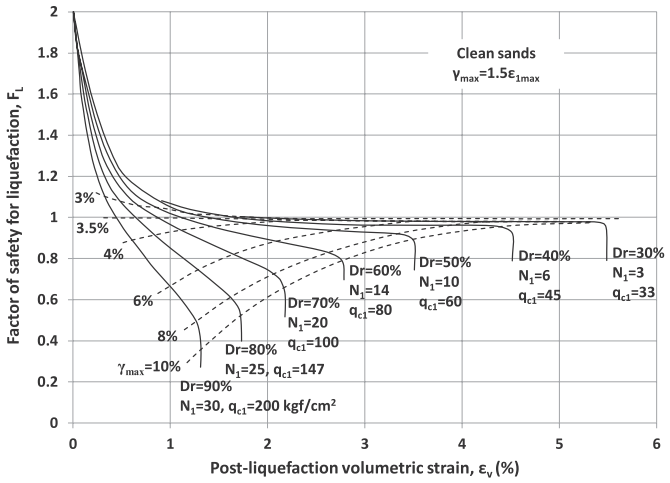

Fig. 2. Estimation of post-cyclic volumetric strain by Ishihara and Yoshimine method [15].

condition are important parameters that influence the particle breakage of calcareous soil [28]. The dynamic properties of calcareous soils obtained from different locations of the Persian Gulf were studied and compared with siliceous soils [33–35]. Previous studies have shown that the cyclic resistance of calcareous deposit is higher than that of siliceous soil [36–38].

This paper presents the results of an experimental study on post-cyclic volumetric strain of calcareous sand collected from the north coast of the Persian Gulf. A series of hollow cylindrical torsional shear tests was performed on Hormuz calcareous sand prepared at different relative densities. The specimens were loaded cyclically under different cyclic stress ratios in undrained condition and then terminated at the desired excess pore water pressure ratios (r_u). After that, the excess pore water pressure was allowed to dissipate, causing the occurrence of volumetric strain. Ultimately, the effects of *Dr*, *CSR*, r_u and γ_{max} on the $\varepsilon_{re,v}$ of the reconstituted sand were evaluated.

2. Soil characterization

The calcareous sand used in this study was obtained from Hormuz Island in the northern shore of the Persian Gulf. Hormuz Island is a historic island, which lies 30 km south east of the Bandar-Abbas commercial port located in the northern coast of the famous Hormuz Strait. This strategic strait is situated between two well-known gulfs, the Persian Gulf and the Gulf of Oman. Fig. 3 shows the location of the Hormuz Island in the Persian Gulf. The grain size distribution analyses and the physical properties of the calcareous sand are shown in Fig. 4 and Table 1, respectively.

Using *HCL* acid and measuring the released gas (i.e., CO_2) resulted from the reaction between carbonates and the acid [39], the carbonate content of Hormuz Island sand (*HI sand*) was found to be approximately 70%. The results of chemical tests showed that about 20% of soil was formed by SiO_2 and about 10% of soil was formed by other compounds such as Fe_2O_3. Consequently, *HI* sand can be categorized as carbonate-rich sand or siliceous carbonate sand [40,41].

Fig. 5 shows the scanning electron microscopic images (*SEM* image) of *HI* sand. The scanned calcareous sand contains thin-walled mollusk, echinoderm plate fragments and thick-walled foraminifera, which are the fauna located in the ocean and seas and has an intra-particle void that can be filled by water or air. It can be inferred from Fig. 5 that *HI* grains are angular and have many voids on a particle surface, which result in high roughness.

3. Sample preparation and testing program

The experimental part of study was performed in the Geotechnical Engineering Research Center (GERC) of Iran University of Science and Technology (IUST) using the hollow cylindrical torsional apparatus (HCTA), which was made by GDS Instruments Company. The HCTA contained 5 main units including pressure/volume controller unit, axial/torsional loading unit, cell pressure (i.e., Plexiglas cell), digital control system and computer unit. More details about the HCTA can be obtained in [42].

The air pluviation method, a method described by Towhata [1], was used for the sample preparation. The dry soil was spread into a hollow

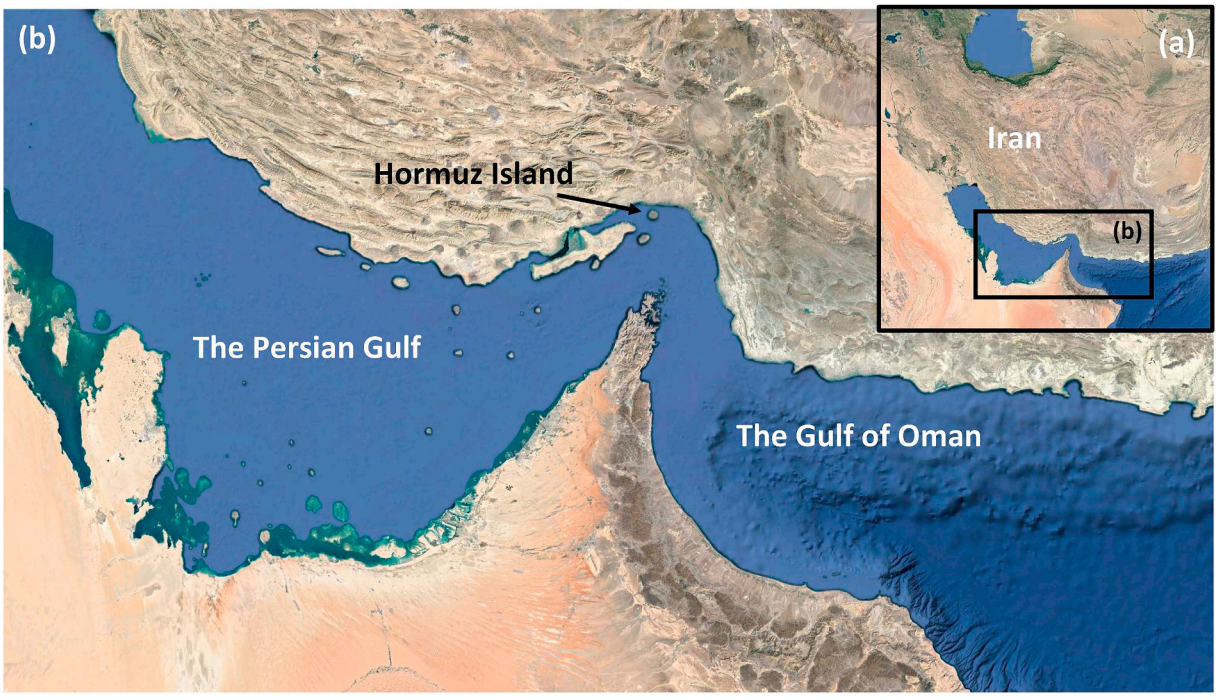

Fig. 3. (a) Map of Iran, (b) The location of Hormuz Island in the Persian Gulf.

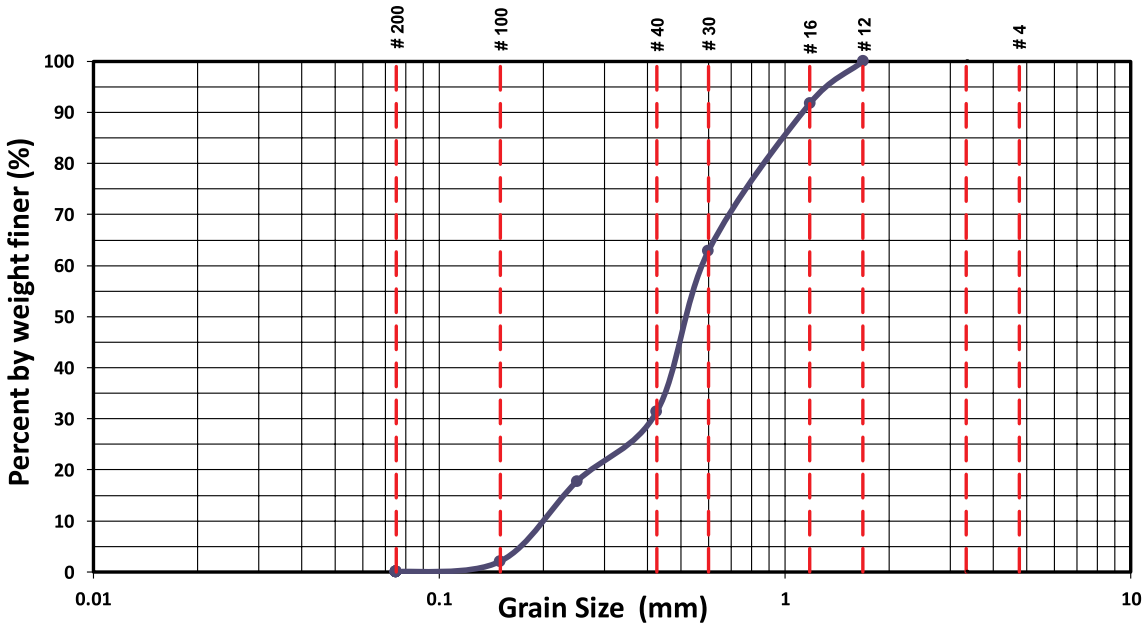

Fig. 4. Grain size distribution of Hormuz Island sand.

Table 1
Physical properties of Hormuz Island sand.

Soil property	Value
Unified soil classification	SP
Coefficient of uniformity, C_u [a]	2.876
Coefficient of curvature, C_c [b]	1.503
Effective grain size, D_{10} (mm)	0.202
Diameter corresponding to 50% finer, D_{50} (mm)	0.521
Specific gravity, G_s	2.930
Minimum void ratio, e_{min}	0.444
Maximum void ratio, e_{max}	0.669
Minimum dry density, $(\gamma_d)_{min}$ (kN/m^3)	17.23
Maximum dry density, $(\gamma_d)_{max}$ (kN/m^3)	19.91

[a] $C_u = D_{60}/D_{10}$.
[b] $C_c = D_{30}^2/(D_{60}*D_{10})$.

cylinder mold in 5 layers to obtain more uniform samples. Each layer had different relative densities, in which the first layer had the least relative density, the middle layer had the target relative density and the last layer had the most relative density. This sample layering method is known as undercompaction and was first proposed by Ladd [43]. The internal and external diameters and the sample heights were approximately 60 mm, 100 mm and 200 mm, respectively.

To achieve the saturation condition, after flushing CO_2 and exuding de-aired water to the specimens, a back pressure of 240 kPa under an effective pressure of 10 kPa was applied to the samples. Using this method of saturation, a B-value greater than 0.96 was obtained in all tests. Calcareous soils have intra-particle voids that never be fully saturated by common saturation methods. However, the saturation conditions in the intra-particle voids do not affect the undrained cyclic behavior of calcareous soil, while the amount of particle breakage is negligible. Subsequently, the samples were isotropically consolidated under 150 kPa. Measuring the volume of withdrawing water from the sample, after consolidation relative density of the specimen (Dr_{ac}) was calculated. The cyclic stress-controlled loading with 0.1 Hz frequency was applied in undrained condition, and the tests were terminated at the desired excess pore water pressure ratio (r_u). After that, the excess pore water pressure was allowed to dissipate, and the post-cyclic volumetric strain was measured.

In this study, the specimens were prepared at three different relative densities including loose, medium and medium-dense conditions.

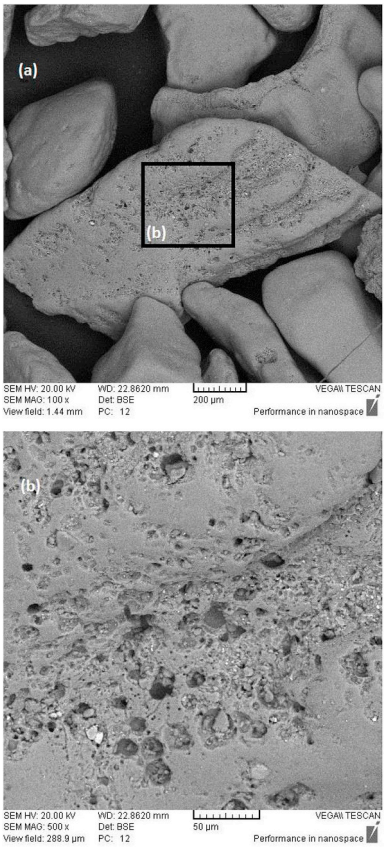

Fig. 5. *SEM* image of the *HI* sand; (a) platy shape and angular particles; b: close-up view of particle which contains intra-particle voids.

Different values of *CSRs*, ranging from 0.25 to 0.625, were applied to the samples in undrained condition. The desired r_u for termination of the tests were 0.4, 0.8 and 1.0 (as initial liquefaction condition). Due to a short delay between the manually termination of the tests by the operator and the termination of torsional shear loading by the apparatus, there are differences between the desired (or target) r_u and the final r_u of each test. Table 2 shows a summary of the tests conducted in

Table 2
Summary of undrained cyclic hollow cylindrical torsional tests.

Test No.	CSR	Dr_{ac} (%)	γ_{max} (%)	N_{cyc}	Final r_u
1	0.250	29.76	0.24	29	0.38
2	0.250	29.61	0.71	67	0.81
3	0.250	29.40	5.82	76	1.00
4	0.325	29.12	0.32	8	0.41
5	0.325	29.60	1.76	18	0.78
6	0.325	30.09	6.76	24	1.00
7	0.400	29.03	0.72	3	0.43
8	0.400	29.48	2.16	8	0.79
9	0.400	29.83	8.01	15	1.00
10	0.475	29.44	1.20	2	0.48
11	0.475	29.52	2.43	3	0.75
12	0.475	29.41	11.47	7	1.00
13	0.325	49.43	0.44	24	0.43
14	0.325	49.49	1.03	82	0.54
15	0.325	49.66	3.96	120	1.00
16	0.400	49.23	0.69	9	0.43
17	0.400	49.42	1.60	38	0.84
18	0.400	49.28	4.14	62	1.00
19	0.475	49.62	1.33	2	0.47
20	0.475	51.40	3.96	11	0.90
21	0.475	50.51	5.02	28	1.00
22	0.550	50.68	2.12	1	0.51
23	0.550	50.38	4.51	8	0.90
24	0.550	49.55	5.46	22	1.00
25	0.400	63.05	0.61	9	0.38
26	0.400	66.86	1.12	63	0.78
27	0.400	63.17	2.59	118	1.00
28	0.475	65.27	0.70	3	0.44
29	0.475	64.76	1.32	19	0.80
30	0.475	64.80	2.78	63	1.00
31	0.550	64.94	1.08	2	0.52
32	0.550	66.21	1.76	9	0.80
33	0.550	66.00	3.27	56	1.00
34	0.625	64.83	1.19	3	0.58
35	0.625	65.30	2.38	9	0.84
36	0.625	64.92	3.86	46	1.00

this study. It should be noted that γ_{max} refers to the maximum single amplitude cyclic-induced shear strain.

4. Results and discussions

4.1. Hollow cylindrical torsional shear test results

As stated before, a series of hollow cylindrical torsional shear tests was conducted on reconstituted samples of Hormuz Island sand. Fig. 6 presents the test results on the *HI* calcareous sand prepared in loose, medium and medium-dense conditions. The specimens were subjected to $CSR = 0.4$ in simple shear mode. The target excess pore water pressure ratio was 1.0 as initial liquefaction condition in these tests. Approximately 15, 62 and 118 cycles were needed in loose, medium and medium-dense reconstituted samples, respectively, for initial liquefaction to occur. The variation of shear stress versus shear strain is shown in Fig. 6a, c and 6e. Obviously, hysteresis stress-strain loops became flattened and shear modulus decreased in undrained stress-controlled condition. Higher values of maximum cyclic-induced shear strain occurred in the specimen prepared at loose condition. The values of γ_{max} were approximately 8%, 4% and 2.5% for loose, medium and medium-dense *HI* samples, respectively. Positive pore water pressure caused the stress path curve to move to the left and reduced the mean effective stress to zero at initial liquefaction (see Fig. 6b, d and 6f). The samples were drained and volumetric strain occurred after the termination of loading. Fig. 7 shows the variations of the post-cyclic volumetric strain of 3 samples prepared at different relative densities. As expected, the ultimate post-cyclic volumetric strain of loose specimen was higher than that of other samples.

To evaluate the effect of important factors including r_u and γ_{max}, on $\varepsilon_{re,v}$, tests with similar conditions of relative densities and stress histories were performed. The loading stage was terminated when the excess pore water pressure ratio reached the different target values (i.e., $r_u = 0.4$, 0.8 and 1.0). Fig. 8a shows the variations of the excess pore water pressure ratio with the number of cycles for three loose samples subjected to $CSR = 0.4$. As seen from this figure, the trends of excess pore water pressure generation coincide with each other. Dissipation of excess pore water pressure resulted in volumetric strain, which is shown in Fig. 8b. The curves shown in this figure correspond to tests performed on the *HI* calcareous specimens that have reached different levels of r_u. It can be concluded that, increasing the excess pore water pressure increases ultimate $\varepsilon_{re,v}$. When r_u reached the unit value (initial liquefaction occurred), the ultimate $\varepsilon_{re,v}$ increased rapidly in comparison to the post-cyclic volumetric strain of the samples with $r_u < 1.0$. Many researchers have stated that failure condition significantly affects the post-cyclic settlement of soil materials [4,14,15].

Particle shape and breakage are two major physical properties, which affect the mechanical behavior of calcareous deposits [23,28,44–46]. Particle size distribution analyses were conducted before and after each test to calculate the amount of particle breakage of the Hormuz calcareous sand. The results showed that due to the low range of confining pressure and shear strain, particle breakage during the tests of this research was negligible. Consequently, grain shape was crucial to the cyclic behavior of the calcareous sand used in this study. Fig. 8a shows that, high pore water pressure relaxation (high fluctuation) occurred between the cycles, which is due to the angular and platy shapes of calcareous deposit [36,45].

4.2. Effect of soil density on post-cyclic volumetric strain

In this study, specimens were prepared at three different relative densities including 30, 50 and 65% to evaluate the effect of soil density on post-cyclic settlement of *HI* calcareous deposits. Fig. 9 shows that the loose specimens presented higher values of ultimate $\varepsilon_{re,v}$ compared to the denser samples. It was stated by previous researches that more settlement occurred at the same level of the cyclic stress ratio (*CSR*) in the ground surface of the soil with lower densities [4,12,15].

4.3. Effects of excess pore water pressure ratio on post-cyclic volumetric strain

To evaluate the effect of r_u on ultimate post-cyclic volumetric strain of *HI* calcareous sand, the specimens were reconstituted at similar relative densities and were loaded at similar cyclic stress ratios. The only difference of these tests was the termination point of loading stage. The relation between r_u and ultimate $\varepsilon_{re,v}$ in loose, medium and medium-dense specimens subjected to $CSR = 0.4$ is showed in Fig. 10 for instance. According to previous researches on siliceous soil such as [4,13–16], the increase of excess pore water pressure increased the ultimate $\varepsilon_{re,v}$. The results showed that the ultimate $\varepsilon_{re,v}$ values increased at higher rate near the liquefaction condition.

4.4. Effect of maximum cyclic-induced shear strain on post-cyclic volumetric strain

As previously stated, shear strain plays a key role in post-cyclic settlement of soil materials. Fig. 11 shows the relation of γ_{max} (single amplitude) and ultimate $\varepsilon_{re,v}$ for samples prepared at different relative densities including 30%, 50% and 65%. Increasing the maximum shear strain during cyclic loading increased the ultimate $\varepsilon_{re,v}$. Initial liquefaction condition (i.e., $r_u = 1.0$) significantly affected the values of γ_{max}. In fact, due to cyclic-induced shear strains experienced by the specimens under relatively low effective stress conditions during previous cyclic loadings, large volume changes at initial liquefaction condition is a reflection of significant changes in the fabric of the soil (i.e., soil particle arrangement) [14]. Table 2 shows the significant increases of

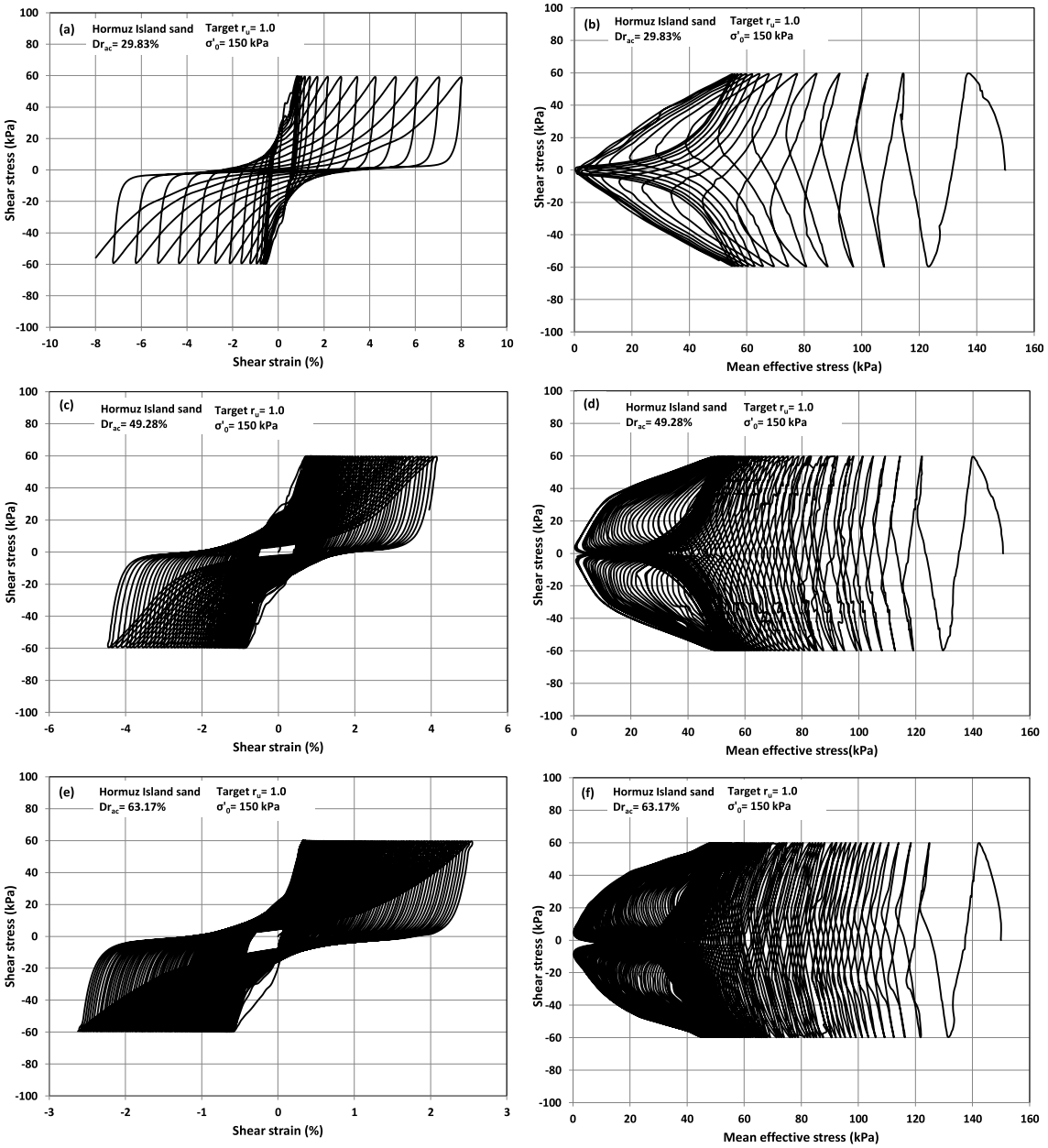

Fig. 6. Results of torsional shear tests on Hormuz Island sand at loose, medium and medium-dense conditions under *CSR* = 0.4; (a): stress-strain curve of loose condition, (b): stress path of loose condition, (c): stress-strain curve of medium condition, (d): stress path of medium condition, (e): stress-strain curve of medium-dense condition, (f): stress path of medium-dense condition.

maximum cyclic-induced shear strain at initial liquefaction conditions (especially for specimens with lower relative densities).

4.5. Effect of cyclic stress ratio on post-cyclic volumetric strain

The reconstituted *HI* samples were subjected to different cyclic stress ratios (i.e., *CSRs*) to evaluate the effect of shear stress on ultimate $\varepsilon_{re,v}$. The results showed that higher ultimate $\varepsilon_{re,v}$ occurred in specimens subjected to higher *CSRs* at a constant r_u (Fig. 10). Evaluating the effect of *CSR* on γ_{max} showed that higher *CSR* results in higher values of γ_{max} at the same excess pore water pressure ratio level (Fig. 11). As stated previously, increasing the maximum cyclic-induced shear strain increases the ultimate $\varepsilon_{re,v}$.

4.6. Comparison of post-cyclic volumetric strain of HI calcareous and siliceous sands

Fig. 12 shows the difference in the relation of ultimate $\varepsilon_{re,v}$ and r_u of *HI* calcareous and several siliceous sands including Fuji River sand [4], Monterey sand [10] and Ottawa sand [17], which were tested previously under relatively similar conditions with this study. Although the variations of ultimate $\varepsilon_{re,v}$ with r_u are similar for both calcareous and siliceous sands and approaching the excess pore water pressure ratio to the unit value increases the ultimate $\varepsilon_{re,v}$ significantly, the ultimate post-cyclic volumetric strain of *HI* calcareous sand is higher than that of siliceous soils for the same value of the excess pore water pressure ratio. As stated by many researchers, particle crushing and particle characteristics (including particle shape and roughness) of calcareous soil

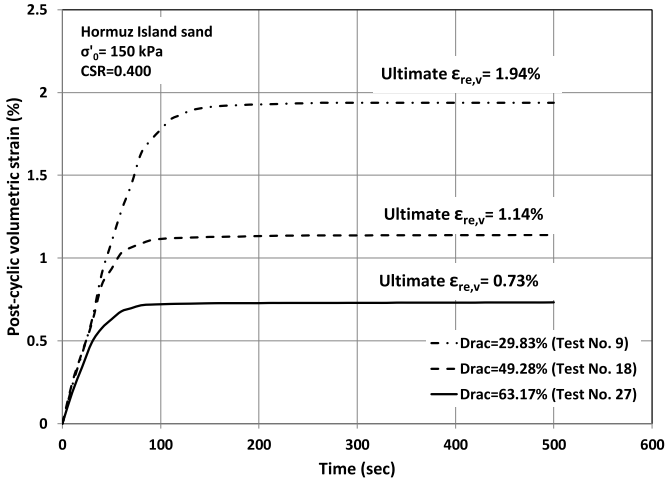

Fig. 7. Post-cyclic volumetric strain of *HI* samples prepared at different relative densities.

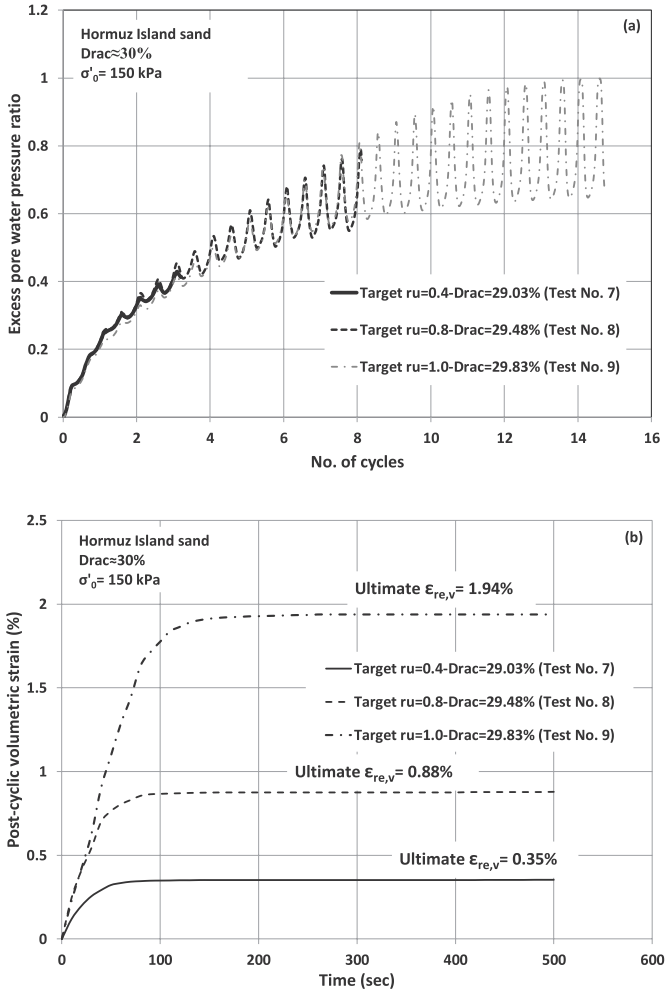

Fig. 8. (a): excess pore water pressure ratio versus No. of cycles in loose samples under *CSR* = 0.4, (b): post-cyclic volumetric strain of loose samples subjected to *CSR* = 0.4.

play important roles in monotonic and cyclic behavior of these sediments [26,48]. Based on the results of sieve analyses before and after of the tests, the particle breakage of *HI* calcareous sand was negligible. The angularity and roughness of the calcareous particles observed in *SEM* images resulted in higher cyclic resistance of *HI* calcareous soil.

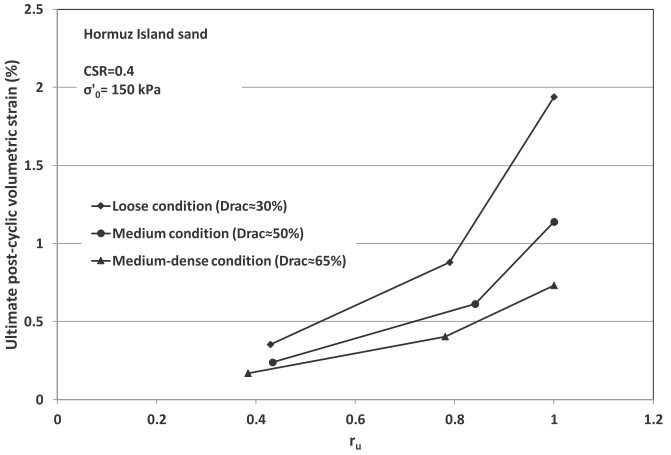

Fig. 9. The effect of relative density on ultimate post-cyclic volumetric strain in *CSR* = 0.4.

Many researchers stated that cyclic strength of calcareous soil is higher than that of siliceous deposits [36,47,49,50]. In other words, increasing excess pore water pressure under cyclic loading is more difficult in calcareous soil. In order to obtain similar r_u values under constant conditions of stress and density, more cycles are required for calcareous sand, which result in higher post-cyclic volumetric strain.

4.7. The most effective factors on post-cyclic volumetric strain

The results of the study showed that relative density, excess pore water pressure ratio, stress state (i.e., cyclic stress ratio and number of cycles) and maximum shear strain all affect the amount of ultimate post-cyclic volumetric strain of calcareous sand. Similarly with siliceous soils, r_u and γ_{max} are two major factors in predicting the ultimate $\varepsilon_{re,v}$ in calcareous deposits. As presented in Figs. 12 and 13, the excess pore water pressure ratio and the maximum cyclic-induced shear strain were used to estimate the ultimate post-cyclic volumetric strain of Hormuz Island sand. A comparison of the figures shows that the most effective factor in estimating the ultimate $\varepsilon_{re,v}$ in a range of $0 \leq r_u < 1.0$ is γ_{max} due to less scattered data in Fig. 13. The key role of shear strain amplitude in the cyclic behavior and volumetric change of soil materials was stated by many researchers [51–53].

5. Conclusion

Dissipation of excess pore water pressure generated during cyclic loadings results in post-cyclic volumetric strain, which causes severe damage to structures. The effects of relative density (*Dr*), cyclic stress ratio (*CSR*), excess pore water pressure ratio (r_u) and maximum shear strain (γ_{max}) on ultimate post-cyclic volumetric strain ($\varepsilon_{re,v}$) of calcareous sand were investigated in this study. The calcareous sand used in this research was obtained from the Hormuz Island in the northern shore of the Persian Gulf. A series of hollow cylindrical torsional shear tests at different initial conditions was performed on reconstituted Hormuz Island sand. The following conclusions were obtained from the study:

1 The excess pore water pressure ratio and the maximum cyclic-induced shear strain are two major factors, that influence the ultimate post-cyclic volumetric strain of *HI* sands. The results show that these parameters are useful for estimating the ground surface settlement.
2 The increase of excess pore water pressure and maximum cyclic-induced shear strain resulted in a higher ultimate $\varepsilon_{re,v}$ value. At initial liquefaction condition (i.e., $r_u = 1$), the specimens became unstable and γ_{max} and ultimate $\varepsilon_{re,v}$ increased rapidly. As an instance, the result of this study at loose condition showed that when r_u

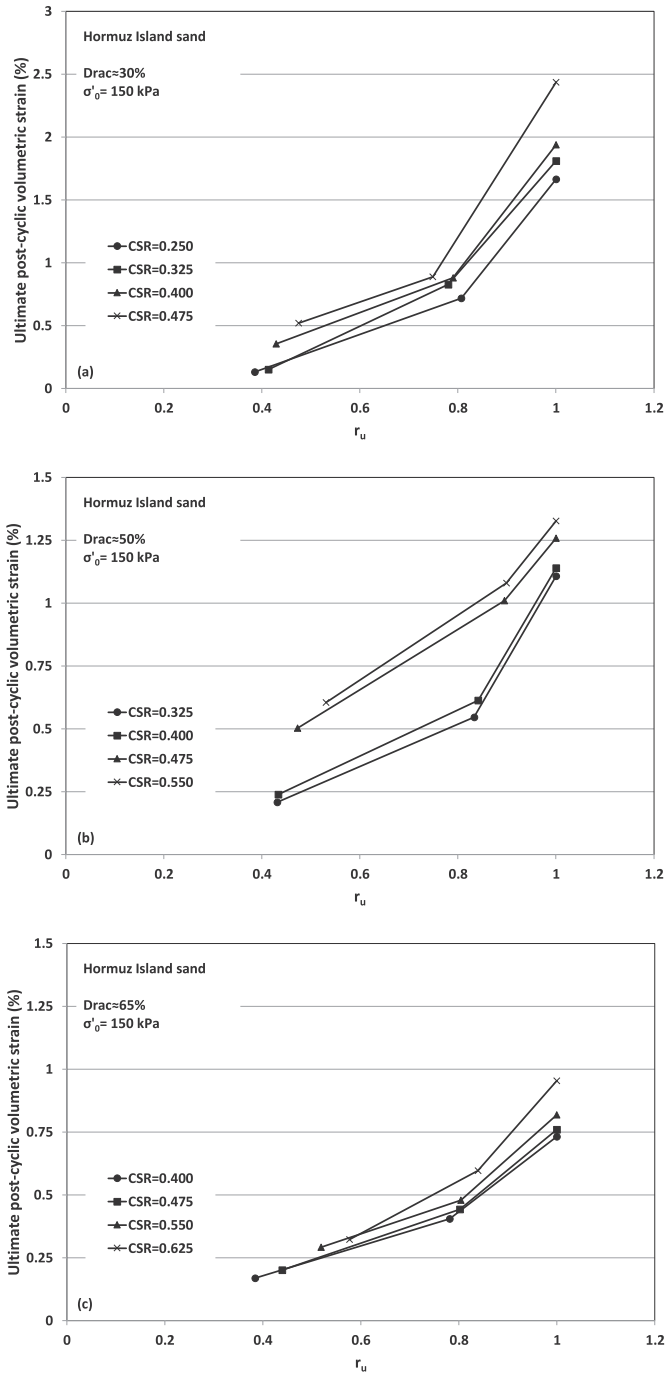

Fig. 10. The relation of excess pore water pressure ratio and ultimate post-cyclic volumetric strain of *HI* samples; (a) loose condition, (b) medium condition, (c) medium-dense condition.

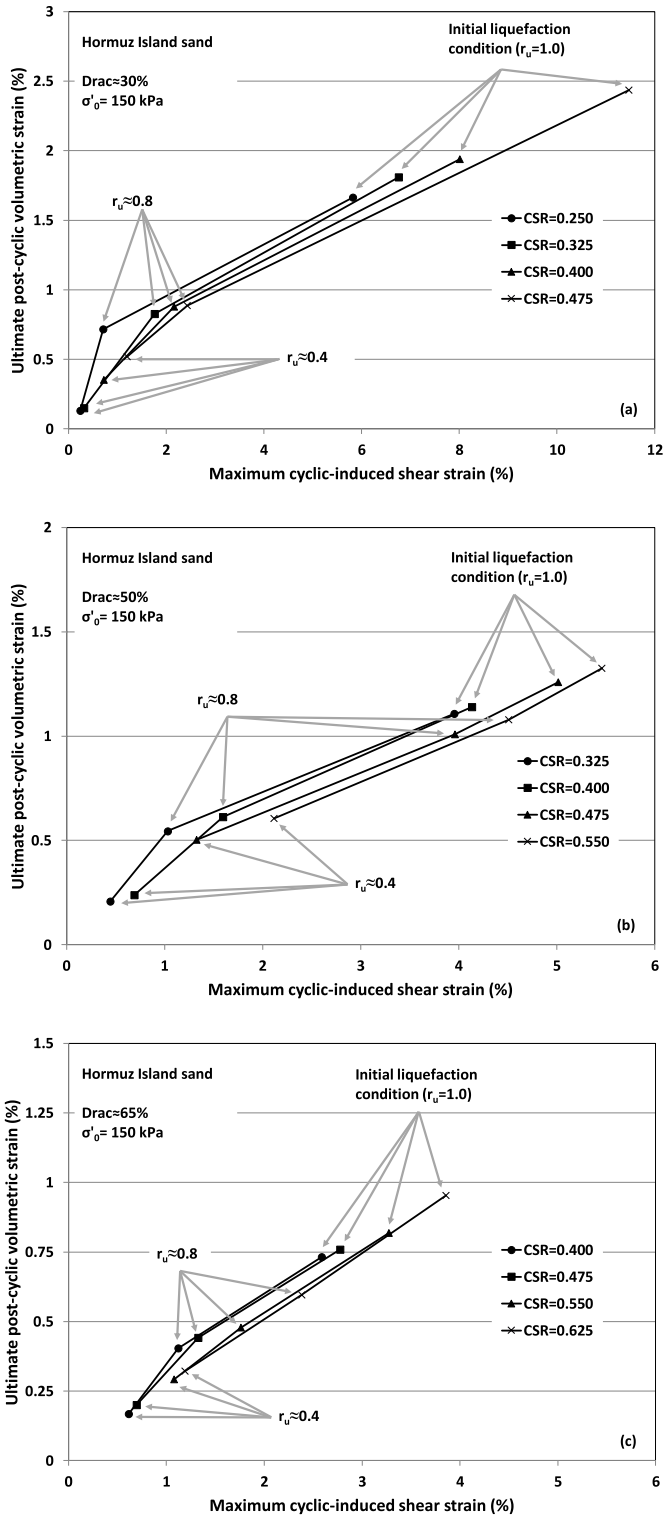

Fig. 11. The relation of maximum cyclic-induced shear strain and ultimate post-cyclic volumetric strain of *HI* samples; (a) loose condition, (b) medium condition, (c) medium-dense condition.

increased from 0.4 to 0.8 (i.e., $\Delta r_u = 0.4$), maximum variations of γ_{max} and $\varepsilon_{re,v}$ were about 1.44% and 0.68%, respectively. On the other hand, when r_u changed from 0.8 to 1.0 (i.e., $\Delta r_u = 0.2$), maximum variations of γ_{max} and $\varepsilon_{re,v}$ were about 9.04% and 1.55%, respectively.

3The relation of ultimate $\varepsilon_{re,v}$ and r_u of *HI* calcareous and siliceous sands showed that higher ultimate post-cyclic volumetric strain occurred in *HI* calcareous soil at constant excess pore water pressure ratio under similar stress states.

4 Exact estimating the ultimate post-cyclic volumetric strain is very difficult and there are many parameters affect the ultimate $\varepsilon_{re,v}$. However, based on the results of this study, the most effective parameter for estimating the ultimate $\varepsilon_{re,v}$ in *HI* calcareous sand was

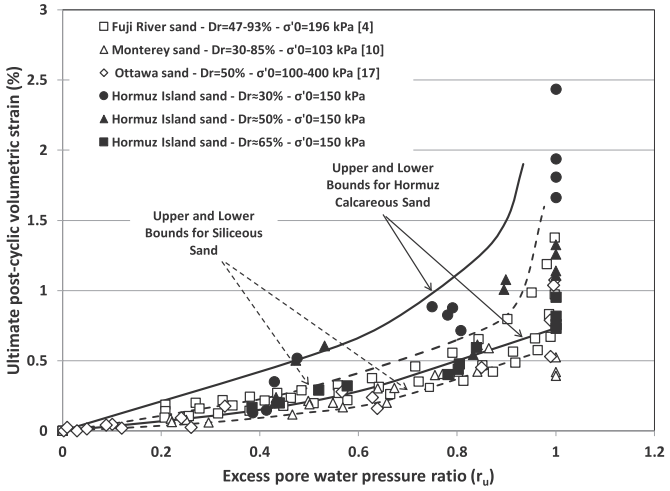

Fig. 12. Comparison of ultimate post-cyclic volumetric strain of calcareous and siliceous sands.

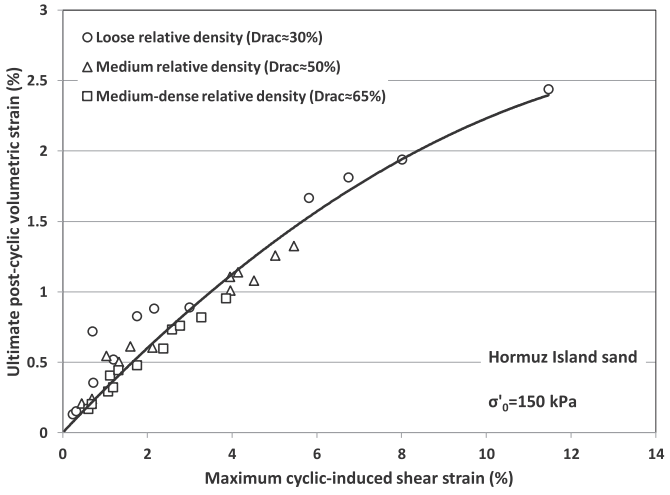

Fig. 13. Variation of ultimate post-cyclic volumetric strain of *HI* samples based on maximum cyclic-induced shear strain.

maximum cyclic-induced shear strain during applying uniform stresses in a range of $0 \leq r_u < 1.0$.

References

[1] Towhata I. Geotechnical earthquake engineering. Berlin: Springer; 2008. p. 684.
[2] Baziar MH, Saeedi Azizkandi A. Evaluation of lateral spreading utilizing artificial neural network and genetic programming. Int J Civ Eng 2013;11(2 B):100–11.
[3] Retamal E, Kausel E. Vibratory compaction of the soil and tectonic subsidence during the 1960 earthquake in Valdevia, Chile. Proc fourth world conf earthq eng. 1969.
[4] Nagase H, Ishihara K. Liquefaction-induced compaction and settlement of sand during earthquakes. Soils Found 1988;28(1):65–76.
[5] Ishihara K, Koga Y. Case studies of liquefaction in the 1964 Niigata earthquake. Soils Found 1981;21(3):35–52.
[6] Iwai TA, Yasui M. Settlement and inclination of reinforced concrete buildings in Dagupan City due to liquefaction during the 1990 Philippine earthquake. Proc 10th world conf earthq eng. vol. 2. Rotterdam, The Netherlands: A.A. Balkema; 1992. p. 147–52.
[7] Japanese Geotechnical Society (JGS). Report on the investigations of the 1999 Kocaeli earthquakes, Turkey 2000. [in Japanese].
[8] Cubrinovski M, Bray JD, Taylor M, Giorgini S, Bradley B, Wotherspoon L, Zupan J. Soil liquefaction effects in the central business district during the february 2011 Christchurch earthquake. Seismol Res Lett 2011;82(6):893–904.
[9] Bhattacharya S, Hyodo M, Goda K, Tazoh T, Taylor CA. Liquefaction of soil in the Tokyo bay area from the 2011 Tohoku (Japan) earthquake. Soil Dynam Earthq Eng 2011;31(11):1618–28.
[10] Lee KL, Albaisa A. Earthquake induced settlements in saturated sands. J Geotech Geoenviron Eng 1974;100(4):387–406.
[11] Tokimatsu K, Seed HB. Simplified procedures for the evaluation of settlements in sands due to earthquake shaking. Rep No UCB/GT-84/16. Berkeley: University of California; 1984.
[12] Tatsuoka F, Sasaki T, Yamada S. Settlement in saturated sand induced by cyclic undrained simple shear. Proc World Conf Earthq Eng 1984;8(3):95–102.
[13] Hyodo M, Yasuhara K, Murata H. Earthquake induced settlements in clays. Proc 9th world conf earthq eng. vol. 3. 1988. Tokyo-Kyoto Japan.
[14] Wijewickreme D, Sanin MV. Postcyclic reconsolidation strains in low-plastic fraser river silt due to dissipation of excess pore-water pressures. J Geotech Geoenviron Eng 2010;136(10):1347–57.
[15] Ishihara K, Yoshimine M. Evaluation of settlements in sand deposits following liquefaction during earthquakes. Soils Found 1992;32(1):173–88.
[16] Shamoto Y, Sato M, Zhang JM. Simplified estimation of earthquake-induced settlements in saturated sand deposits. Soils Found 1996;36(1):39–50.
[17] Omarov M. Liquefaction potential and post-liquefaction settlement of saturated clean sands: and effect of geofiber reinforcement MSc thesis University of Alaska Fairbanks; 2010
[18] Tokimatsu K, Seed HB. Evaluation of settlements in sands due to earthquake shaking. J. Geotech. Eng. 1987;113(8):861–78.
[19] Shamoto Y, Zhang JM, Tokimatsu K. Methods for evaluating residual post-liquefaction ground settlement and horizontal displacement. Soils Found 1998;38:69–84.
[20] Yi F. Procedure to evaluate liquefaction-induced settlement based on shear wave velocity. 9th US natl and 10th Canadian earthq eng reaching beyond borders. 2010. p. 291.
[21] Yoshimine M, Nishizaki H, Amano K, Hosono Y. Flow deformation of liquefied sand under constant shear load and its application to analysis of flow slide of infinite slope. Soil Dynam Earthq Eng 2006;26(2):253–64.
[22] Holmes A. Principles of physical geology Sunbury-on-Thames, Nelson, London 1978. p. 730.
[23] Coop M. The mechanics of uncemented carbonate sands. Geotechnique 1990;40(4):607–15.
[24] Morioka BT. Evaluation of the static and cyclic strength properties of calcareous sand using cone penetrometer tests PhD thesis University of Hawaii at Manoa; 1999
[25] Dehnavi Y, Shahnazari H, Salehzadeh H, Rezvani R. Compressibility and undrained behavior of Hormuz calcareous sand. Electron J Geotech Eng 2010;15(O):1684–702.
[26] Shahnazari H, Salehzadeh H, Rezvani R, Dehnavi Y. The effect of shape and stiffness of originally different marine soil grains on their contractive and dilative behavior. KSCE J Civil Eng 2014;18(4):975–83.
[27] Sharma SS, Ismail MA. Monotonic and cyclic behavior of two calcareous soils of different origins. J Geotech Geoenviron Eng 2006;132(12):1581–91.
[28] Shahnazari H, Rezvani R. Effective parameters for the particle breakage of calcareous sands: an experimental study. Eng Geol 2013;159(0):98–105.
[29] Hyodo M, Nakata Y, Aramaki N, Hyde AFL, Inoue S. Liquefaction and particle crushing of soil. Proc 12h world conf earthq eng. 2000. Auckland, New Zealand.
[30] Aghajani HF, Salehzadeh H, Rezvani R. Energy equilibrium during crushing of sandy soils under isotropic compression. Arabian J Sci Eng 2016;41(4):1531–42.
[31] Rezvani R, Shahnazari H, Salehzadeh H, Dehnavi Y. The comparison of monotonic behaviors of two different calcareous sands. Proc First Int Conf Geotech Constr Mater Environ Mie Japan. 1. 2011. Nov.21–23.
[32] Shahnazari H, Rezvani R, Tutunchian MA. Experimental study on the phase transformation point of crushable and noncrushable soils. Mar Georesour Geotechnol 2017;35(2):176–85.
[33] Jafarian Y, Javdanian H, Haddad A. Strain-dependent dynamic properties of Bushehr siliceous-carbonate sand: experimental and comparative study. Soil Dynam Earthq Eng 2018;107:339–49.
[34] Jafarian Y, Javdanian H, Haddad A. Dynamic properties of calcareous and siliceous sands under isotropic and anisotropic stress conditions. Soils Found 2018;58(1):172–84.
[35] Javdanian H, Jafarian Y. Dynamic shear stiffness and damping ratio of marine calcareous and siliceous sands. Geo Mar Lett 2018;38(4):315–22.
[36] Morioka BT, Nicholson PG. Evaluation of the liquefaction potential of calcareous sand. Proc Int Offshore Polar Eng Conf Seattle WA USA. 2000. p. 494–500.
[37] Brandes HG, Seidman J. Dynamic and static behavior of calcareous sands. 18th Int Offshore Polar Eng Conf, Vancouver, Canada. 2008. p. 1–6. Paper No. 2008-TPC-400.
[38] Shahnazari H, Jafarian Y, Tutunchian M, Rezvani R. Probabilistic assessment of liquefaction occurrence in calcareous fill materials of Kawaihae Harbor, Hawaii. Int J Geomech 2016;16(6):05016001.
[39] BSI (British Standards Institute). BS1377: Part 3 chemical and electro-chemical tests. BSI London; 1990.
[40] Beringen F, Kolk HJ, Windle D. Cone penetration and laboratory testing in marine calcareous sediments. ASTM Int 1982;777:179–209.
[41] King RW, Van Hooydonk WR, Kolk HF, Windle DW. Geotechnical investigations of calcareous soils on the North West Shelf, Australia. Offshore Technology conference. Houston, Texas, Offshore Technology Conference. vol. 12. 1980.
[42] Aghajani HF, Salehzadeh H. Anisotropic behavior of the Bushehr carbonate sand in the Persian Gulf. Arab J Geosci 2015;8(10):8197–217.
[43] Ladd RS. Preparing test specimens using undercompaction. Geotech Test J 1978;1(1):16–23.
[44] Datta M, Gulhati S, Rao G. Crushing of calcareous sands during shear. 11th Annu OTC Houston. 1979. p. 1459–60.
[45] Hyodo M, Aramaki N, Nakatay Y, Inoue S, Hyde AFL. Particle crushing and undrained shear behaviour of sand. Cupertino CA ETATS-UNIS. Int Soc Offshore Polar Eng; 1999.

[46] Coop M, Sorensen KK, Freitas TB, Georgoutsos G. Particle breakage during shearing of a carbonate sand. Geotechnique 2004;54(3):157–64.
[47] Ross MS, Nicholson PG. Liquefaction potential and cyclic loading response of Calcareous Soils. University of Hawaii College of Engineering Department of Civil Engineering; 1995.
[48] Zhou XZ, Chen YM, Li WW, Liu HL. Monotonic and cyclic behaviors of loose anisotropically consolidated calcareous sand in torsional shear tests. Mar Georesour Geotechnol 2018 1:14.
[49] Hyodo M, Tanimizu H, Yasufuku N, Murata H. Undrained cyclic and monotonic triaxial behaviour of saturated loose sand. Soils Found 1994;34(1):19–32.
[50] Shahnazari H, Jafarian Y, Tutunchian MA, Rezvani R. Undrained cyclic and monotonic behavior of Hormuz calcareous sand using hollow cylinder simple shear tests. Int J Civ Eng 2016:1–11.
[51] Dobry R, Ladd RS, Yokel FY, Chung RM, Powell D. Prediction of pore water pressure buildup and liquefaction of sands during earthquakes by the cyclic strain method. National Bureau of Standards Building Science Series 138 Gaithersburg, Md: National Bureau of Standards and Technology; 1982. p. 150.
[52] Ladd RS, Dobry R, Dutko P, Yokel FY, Chung RM. Pore-water pressure buildup in clean sands because of cyclic straining. Geotech Test J 1989;12(1):77–86.
[53] Hsu CC, Vucetic M. Volumetric threshold shear strain for cyclic settlement. J Geotech Geoenviron Eng 2003;130(1):58–70.